

1 **Formation of Microcapsules by Ultrasound Stimulation for Use**
2 **in Remote-controlled Drug-eluting Stents**
3

4 **Authors**

5
6 **Wei Yao^a, Yan Bao^a, Yu Chen^b**

7 *^a Department of Biomedical Engineering, The University of Strathclyde, Glasgow , United Kindgom*

8 *^b Department of Physics, The University of Strathclyde, Glasgow , United Kindgom*

9
10 **Corresponding Author**

11 Wei Yao

12 Wolfson Centre

13 Department of Biomedical Engineering

14 University of strathclyde

15 Glasgow G4 0NW

16 UK

17 Email: w.yao@strath.ac.uk

18
19 **Word count: 5000**

20

21

22

23

24

25

26 **Abstract**

27 Coronary Heart Disease (CHD) is the leading cause of death globally. The placement of drug-eluting
28 stents (DESs) in diseased coronary arteries is the most successful minimally-invasive intervention to
29 treat CHD. The key limitations of such interventional therapy are the risk of in-stent restenosis (ISR)
30 and late stent thrombosis. This paper investigates a new drug-release system by formatting
31 nanoparticles as drug carriers, which are later subjected to an external ultrasonic stimulus for
32 controlled drug release remotely for DESs. The drug delivery could delay smooth muscle cell growth
33 whilst enabling effective regeneration of a functional endothelium. Microcapsules were produced by
34 employing a layer-by-layer technique, encapsulated with Rhodamine 6G dye used in place of anti-
35 restenotic drugs. Gold nanoparticles were employed as a shell in the microcapsules. The presence of
36 gold nanoparticles significantly enhanced the efficiency of the ultrasonically induced dye release from
37 the microcapsules and increased the sensitivity of the microcapsules to ultrasonic stimulation
38 compared to those without gold nanoparticles.

39

40 **Keywords:** Drug-Eluting Stent, Remote Control, Nano-particle

41

42

43

44

45

46

47

48

49 **1. Introduction**

50 Coronary Heart Disease (CHD) is a global health challenge, resulting in around 17.3 million deaths
51 annually [1]. The placement of stents in diseased coronary arteries is the most successful minimally-
52 invasive intervention to treat CHD. The most advanced stents are drug-eluting stents (DES), which
53 release a drug to inhibit the excessive smooth muscle proliferative process responsible for the
54 inconsistent results achieved with bare metal stents. However, there is evidence that DES prevent
55 regrowth of the endothelial cell layer (endothelium) that lines the innermost layer of the artery and it is
56 increasingly clear that regeneration of this layer is crucial to securing positive long term outcomes [2].
57 There is thus a need for a stent that inhibits smooth muscle cell growth whilst enabling effective
58 regeneration of a functional endothelium. Current DES drug release profiles lead to high initial anti-
59 proliferative drug concentrations within the artery wall, which slowly decay over weeks and months [3].
60 However, the process of endothelial regeneration is thought to occur within the first few days following
61 bare metal stent implantation [4], whilst the excessive smooth muscle cell proliferation response is
62 significantly delayed and occurs over weeks and months [5]. In this context, it is perhaps not surprising
63 that existing DES have been associated with incomplete regeneration of the endothelium. Any drug
64 delivery which could delay drug release until after the endothelium had fully healed would therefore be a
65 significant advance. The aim of the research is to investigate ultrasound activated nanoparticles as a
66 means of achieving this, with drug being released into the artery wall when it is most needed.

67

68 However, in-stent restenosis (ISR) remains a serious problem following implantation. The major reason
69 for ISR is the injured arterial wall causing smooth muscle cell (SMC) proliferation and scar tissue
70 accumulation [6]. Meanwhile, drug release happens spontaneously after implantation and often is

71 uncontrolled [7]. To cope with this problem, nanocapsules combined with a drug delivery system can
72 enable drug release in a specific site, as requirements [8-10].

73

74 Stimuli-responsive nanocapsules can release the drug in a controlled manner and the non-invasive nature
75 of the technique has advantages in therapeutic application, such as reduced possibility of infection,
76 avoided damage to surrounding tissues by devices. Most of the literature on nanoparticulate carrier
77 systems is based on the employment of lipid, polymeric, different types of nanoparticulate carriers, and
78 self-assembling carriers [10]. In general, the layer-by-layer assembly of nanocapsules shows advantages:
79 it achieves the integration of component materials from different nature within the films, and it makes the
80 incorporation of various biomolecules into the films. The layer-by-layer technique consists of
81 renaturation of polyion adsorption, allowing the alternation of the terminal charge after each subsequent
82 layer deposition. Furthermore, it achieves a defined control over the thickness, structure, mechanical
83 characteristics and composition of assembled materials [11].

84

85 Gold nanoparticles (AuNP) have been studied for many years in applications such as cancer treatment
86 [12]. They have high biocompatibility, ease of surface modification, facile synthesis, and tuneable optical
87 characteristics [13]. Based on previous research, the release efficiency was investigated by coating gold
88 nanoparticles in the microcapsules shell [14]. When subjected to ultrasound, the microcapsule wall
89 undergoes a morphological change due to shear forces due to the ultrasonic oscillations. If the ultrasonic
90 wavelength correlates to the microcapsule's size, it can maximise the effect. At 1 MHz, the wavelength
91 closes to the size of PE microcapsules [15]. With the introduction of a rigid material such as the AuNP,
92 the higher amount of the embedded nanoparticles leads to a decreased Young's modulus and
93 microcapsule shell elasticity [16]. This can influence the fracture rate under ultrasonic triggering, making

94 them more vulnerable to ultrasound. In addition, the gold nanoparticles are inert and are non-toxic, so
95 they are a feasible material for medical applications. Moreover, the mechanical properties of gold
96 nanoparticles also perform well making the microcapsules relative stable [17, 18].

97

98 Ultrasound is an effective external stimulation that can induce encapsulated drug delivery in vivo [19].
99 Therefore, ultrasound can act upon biomolecules. Ultrasound-responsive polymers for drug delivery
100 systems have been studied in medical diagnostics and treatment [20]. Some polymeric systems that
101 respond to ultrasound are mainly polymeric micelles, gels or other layer-by-layer (LbL) coated
102 nanoparticles. Langer et al., have studied the release rate of incorporated components through the
103 stimulation of ultrasound from polymers, including polylactides, biodegradable polyglycolides and
104 ethylene-vinyl acetate copolymers [21-27]. It has been shown that ultrasonic stimulation can facilitate the
105 permeation through some polymers with no erosion and enhance the decomposition rate in some
106 biodegradable polymers [28][29]. Miyazaki et al. studied the ethylene-vinyl alcohol (EVAL) copolymer
107 and insulin in diabetic rats and were able to control insulin release through the ultrasonic stimulation
108 [30]. Receiving implants encapsulating insulin produced an ultrasonic stimulation (1MHz, 1 W/cm²) and
109 a significant decrease in the level of blood glucose was observed. The results demonstrated a rapid rate of
110 release of insulin in the targeted region. In previous research of this group, they also demonstrated that
111 the release rate of 5-fluorouracil from an EVAL copolymer can rise at desired times upon the ultrasonic
112 stimulation in vivo [31]. Ultrasonic stimulation can induce the collapse of drug carriers and achieve
113 payload release for the uptake of target cells. The site specificity can be promoted by incorporating a
114 surface ligand on the carrier, which is able to bind to specific receptors for specific targeting [32][33].

115

116

117 **2. Methods**

118 **2.1.Synthesis of polylactic acid (PLA) microcapsules**

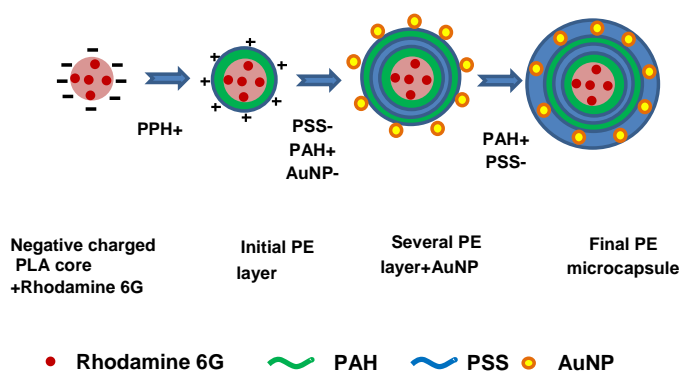
119 The work in this research is an attempt to develop a smart drug nanostructured delivery system that is
120 controllable using ultrasonic stimulation. This research focused on the polyelectrolytes like Polylactic
121 acid (PLA), Poly(allylamine hydrochloride) (PAH), and Poly(styrene sulfonate) (PSS) because of their
122 feasibility and their ability to function as a drug carrier. Rhodamine 6G, a kind of fluorescein dye, loaded
123 in microcapsules was used as a drug surrogate in this model system for the controlled release studies.

124

125 The core of the microcapsule was made up of PLA microparticles. PLA microcapsules were achieved by
126 using the nanoprecipitation method and this method has been introduced in previous research [34]. The
127 main procedure to generate PLA/Rhodamine 6G microcapsules was to dissolve PLA in acetone and
128 equilibrate for 12 hours at room temperature. Next, Rhodamine 6G was added to the acetone solution.
129 Gradually, the colour changes of an acetone solution were observed from colourless to bright red due to
130 the Rhodamine 6G becoming dissolved. The organic solution was stirred to allow the PLA and the
131 Rhodamine 6G to become completely attached. After stirring, the organic solution was added drop by
132 drop into distilled water containing no surfactant, with appropriate stirring for 2 hours. After injecting the
133 organic phase into the aqueous phase, a conspecific microdispersion was obtained. The PLA
134 microcapsules were suspended in water through centrifugation. The PLA/Rhodamine 6G capsules served
135 as the cores of the microcapsules for the next layer-by-layer assemblies. The Rhodamine 6G dye served
136 as a tracer material in place of anti-restenotic drugs. It can be easily detected using fluorescence
137 spectroscopy.

138

139 The layers coated on the PLA cores contain PAH polymers (positive charged), PSS polymer (negative
 140 charged) and citrate stabilized gold nanoparticles (negative charged). With the opposite charge on
 141 polyelectrolytes, the microcapsules can be formed and the number of layers can be varied as required.
 142 Zeta potential measurement was employed to assess the layer-by-layer assembly process. In terms of the
 143 remote ultrasonic stimulation process, the microcapsules suspended in liquid can be stimulated. In the
 144 further clinical application, the system aims to allow the drug release from DES to occur in a controllable
 145 manner.



146
 147 Figure 1 The layering processes of microocapsules.
 148
 149 The grey sphere represents the PLA microo-cores; the pink dots represent the Rhodamine 6G which
 150 serves as a tracer material in place of anti-restenotic drugs; the green layer represents the PAH layer
 151 which is positive charged; the blue layer represents the PSS layer which is negative charged; the gold
 152 layer represents the gold nanoparticles which are negative charged. PLA microcapsules consist of a PLA
 153 core, PAH, PSS and gold nanoparticles shells fabricated by a layer-by-layer assembly technique. In brief,
 154 a 37.5 mL of PAH (1 mg/ml) aqueous solution was added to 25 mL of the PLA and stirred for 2 hours.
 155 The solution was centrifuged for 15 minutes at 13000 rpm and the supernatant was removed. The PAH
 156 coated microcapsules were resuspended in 31 mL of distilled water for the next layer assembly. For the

157 second polyelectrolyte layer coating, 46.5 ml of PSS (1 mg/ml) was added to the above solution and
158 stirred for 2 hours. After centrifuging employing the same parameters, PAH/PSS coated microcapsules
159 were re-suspended in 38 ml of distilled water. The third layer of PAH was assembled following the same
160 process and the PLA-Rh6G/PAH/PSS/PAH microcapsules were again redispersed in 47 ml of water.
161 Next 28.2 mL of citrate stabilized gold nanoparticles (25 mM, synthesized by the sodium citrate
162 reduction method [35]), was added and was vigorously stirred for 2 hours. Following centrifugation and
163 re-suspension, the last layer of PAH was assembled in the same way. Finally PLA-Rh6G
164 /PAH/PSS/AuNP/PAH core-shell structure composite microcapsules were obtained after centrifugation
165 and re-suspension, ready for the ultrasonic stimulation experiments.

166

167 **2.2. Ultrasonic stimulation**

168 In this research, the trigger mechanism was remotely stimulated with ultrasound at a frequency of 1MHz,
169 which poses no harm for the human body within a safe range of frequency. In this research, a hand-held
170 ultrasound device with a frequency of 1 MHz was employed for the stimulation of PLA-Rh
171 6G/PAH/PSS/PAH/AuNP/PAH microcapsules. The technology of therapeutic ultrasound is a high
172 frequency sound vibration which cannot be felt by humans, and can stimulate tissue up to 5 cm beneath
173 the skin's surface. The transducer used in the experiment is a therapeutic ultrasound device
174 ULTRALIEVE made by Actegy Ltd UK. The effective intensity that represents the amount of energy
175 transferred to the tissues is 2.4W/cm². Power supply input is at AC 100-240V 50/60Hz, 0.35A. The size
176 of the transducer is 34mm diameter × 10mm high and the effective radiating area is 4cm².

177

178 It is generally tissues or microcapsules which contain components that are sensitive to the effects of heat.
179 Abnormalities in biochemical processes may appear following the increase of temperature above the

180 normal basal levels. Normally, the heat generated by ultrasound is mostly absorbed by blood circulation
181 *in vivo*, and some heat is distributed through adjacent tissues. Therefore, the heat imparted onto body
182 tissue should be given further attention, otherwise, some tissues or cells will be destroyed . The ultrasonic
183 stimulation process in this project was not active for a long period of time to avoid overheating the
184 microcapsules. In this project, the frequency of medical device was 1MHz, which meets the safety
185 requirement in human body application.

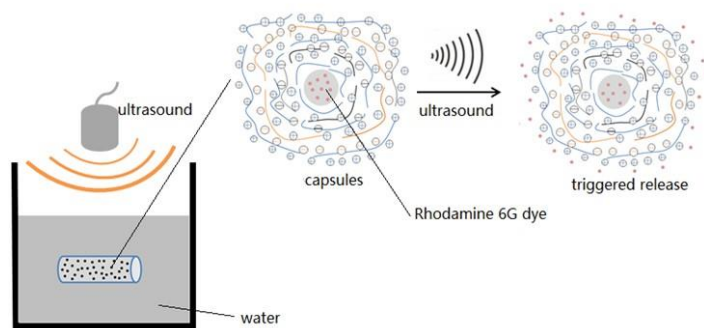
186
187 The duty cycle contains three different levels including Low (30% duty cycle, 0.75W/cm²), Medium
188 (40% duty cycle, 1.0W/cm²) and High (50% duty cycle, 1.2W/cm²). The duty cycle is defined as the
189 percentage during one period in which the signal is active [36-37]. A schematic diagram of the ultrasonic
190 stimulation imparted onto the microcapsules is shown in Figure 2.

191
192
$$D=T/P\times 100\% \tag{1}$$

193
194 In Equation 1, D represents duty cycle, T(μ s) represents the duration of active signal, and P(μ s)
195 represents total duration of signal. For example, a 30% duty cycle pulsed waveform would have
196 ultrasound on for a total of 30% of the entire treatment, and off for a total of 70%. A 100% duty cycle is
197 the same of “continuous”. The device used in this research, the duty cycle is fixed which includes 30%,
198 40% and 50%.

199
200
201
202

203
204
205
206
207
208
209



210 Figure 2 Schematic diagram of the ultrasonic stimulation imparted onto the microcapsules.

211

212 The PLA-Rh6G/PAH/PSS/PAH/AuNP/PAH microcapsules were suspended in the tube and the tube was
213 fixed in water. The ultrasound device was fixed and kept working, which is shown on the left of figure 2.

214 In the microcapsules details shown on the right of figure 2, the gray spheres represent the PLA
215 microcapsules, the red particles represent Rhodamine 6G dye, the blue curves represent the PAH layer
216 (positive charged), the black curves represent the PSS layer (negative charged), and the yellow curves
217 represent the AuNP shell. The dye is released by the stimulation of ultrasound.

218

219 In the future, these drug-loaded microcapsules will be planned to apply to the stents, allowing for a
220 stimuli-response to ultrasound.

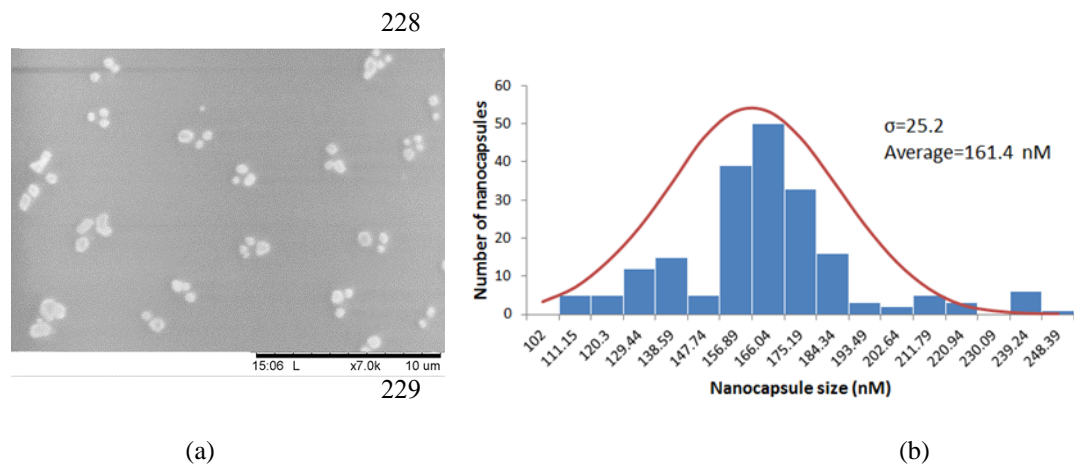
221

222 **3 Results**

223

224 **3.1 SEM analysis microcapsules**

225 PLA-Rh6G /PAH /PSS /PAH /AuNP / PAH/ microcapsules were prepared by an alternating deposition
226 of cationic polymers (PAH) and anionic polymers (PSS) onto the PLA cores doped with Rh6G. An SEM
227 image of the microcapsules is shown in Figure 3.



230 (a) SEM image of PLA-Rh6G/PAH/PSS/PAH/AuNP/PAH microcapsules. (b) The size distribution of microcapsules.

231 Figure 3. SEM image of PLA-Rh6G/PAH/PSS/PAH/AuNP/PAH microcapsules. (a) SEM image of
232 PLA/Rh6G/PAH/PSS/PAH/AuNP/PAH microcapsules. (b) The size distribution of microcapsules.

233

234 Figure 3 shows that the majority of the microcapsules have dispersed spherical shapes with an average
235 size of 165 ± 25 nm (200 microcapsules were accounted).

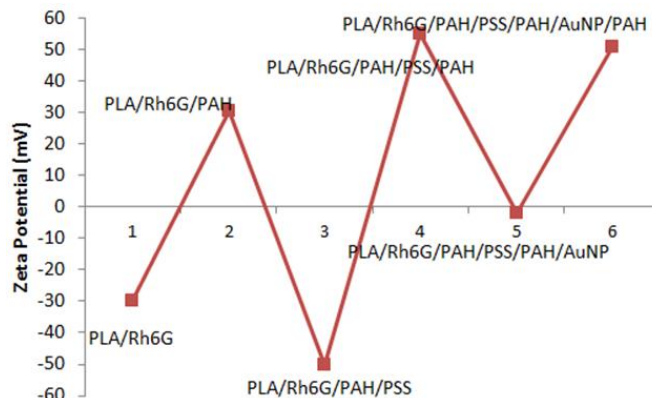
237 3.2 Characterisation of the microcapsule assemblies

238

239 In this research, the microcapsules were synthesized with four polymer layers and one AuNP layer,
240 which contained opposite charges, via layer-by-layer self-assembly processes. To examine the layer-by-
241 layer assembly of PAH, PSS and AuNP on the PLA microcapsules, the sequential assembly procedures
242 were monitored by means of zeta potential of the microcapsules. The variation of zeta potential with the
243 sequential adsorption of the polyelectrolyte layer for the PAH/PSS/PAH/AuNP/PAH coatings is shown
244 in Figure 4.

245

246



247

248

249 Figure 4. Zeta potential measurements in the layer-by-layer assembly of the micro-capsules.

250

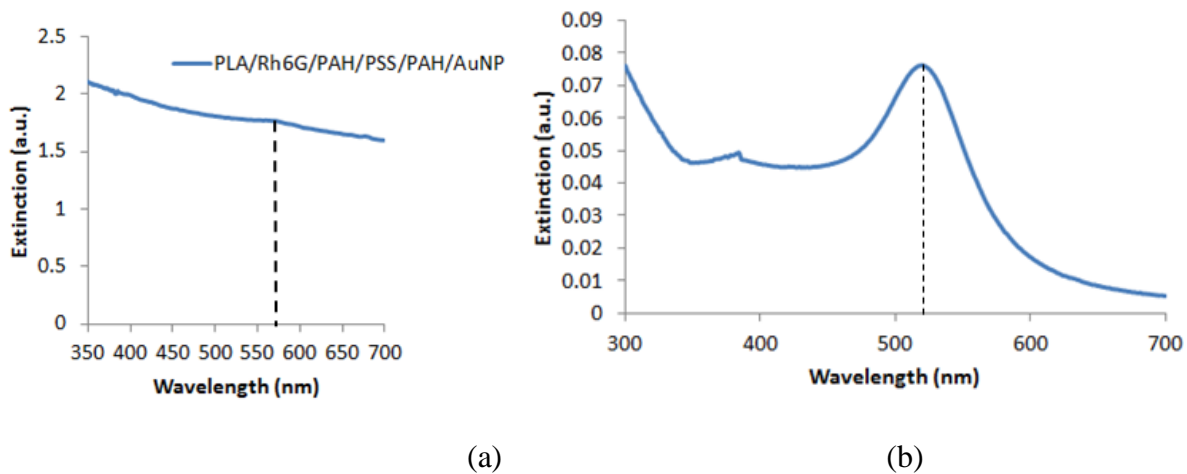
251 The zeta potential value of the pristine PLA microcapsules was negative (-34.5 mV). This is believed to
252 be due to the carboxylic groups present at the surface of the PLA microcapsules [38]. It was observed
253 from the zeta potential measurements that the adsorption of a positively charged PAH layer on the PLA-
254 Rh6G microcapsules changed the zeta potential from -34.5 mV to +30.4 mV. Subsequently, the
255 deposition of a PSS layer led to another potential reversal from +30.4 to -50 mV. Further alternating
256 deposition of the PAH, AuNP and PAH led to continuous reversals in zeta potentials. This revealed a
257 stepwise layer assembly during the fabrication of the composite microcapsules.

258

259 The UV-vis spectrum of the PLA-Rh 6G/PAH/PSS/PAH/AuNP microcapsules is shown in Figure 5. An
260 absorption band due to the surface plasmon resonance of gold nanoparticles was observed indicating the
261 presence of gold nanoparticles in the microcapsules. A red-shift of the surface plasmon band from 519
262 nm shown in Figure 5(b) to 556 nm in figure.5 (a) may possibly be due to the aggregation of the gold
263 nanoparticles when they were assembled onto the microcapsules. This absorption overlaps with a slope

264 of scattering from the large microcapsules. The absorption of Rhodamine 6G (526 nm) is not visible here
265 because it overlaps with the strong scattering of the micro-capsules and also the absorption band of the
266 gold nanoparticles.

267



268

269

270

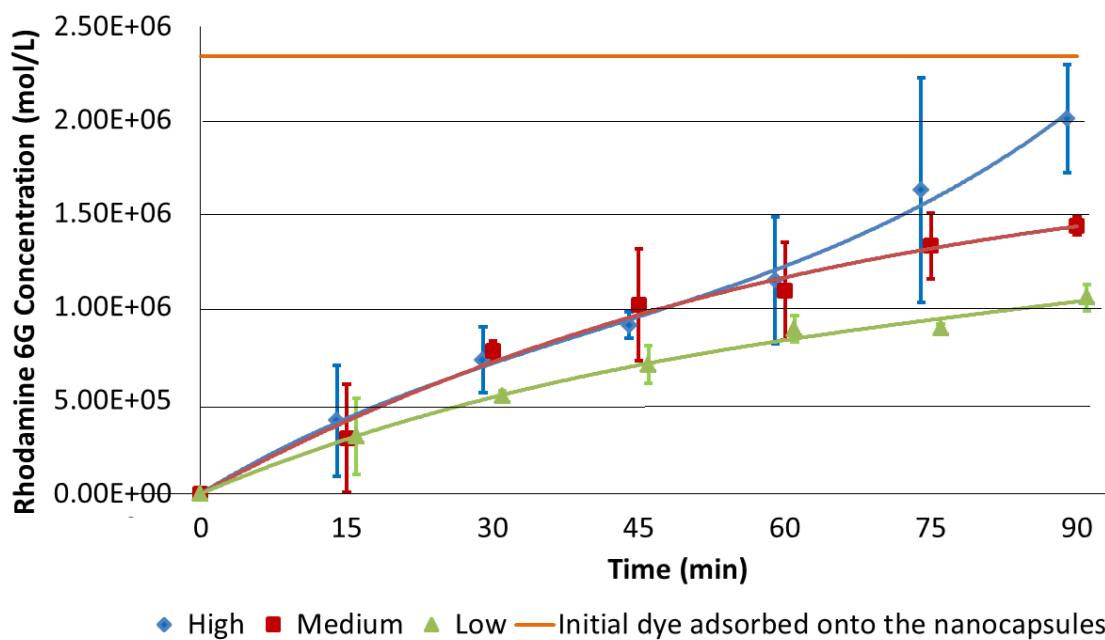
271 Figure 5. (a) Extinction spectrum of the PLA/Rh6G/PAH/PSS/PAH/AuNP/PAH micro-capsules (556nm). (b) UV-vis
272 extinction spectrum of colloidal gold nanoparticles (519nm).

273

274 3.3 Ultrasonic stimulation of the microcapsules

275 The release of Rhodamine 6G dye from the microcapsules after each ultrasonic stimulation was
276 examined via the measurement of concentration of Rh6G in the supernatants. Both the samples and the
277 control samples (microcapsules without gold nanoparticles) undergo ultrasonic stimulation at three
278 different duty cycles. Figure 6 shows the fluorescence intensity change of the dye released from the PLA-
279 Rh6G/PAH/PSS/PAH/AuNP/PAH microcapsules against the ultrasonic stimulation times of the different
280 duty cycles. The measurement was taken after each 15 minutes of stimulation.

281



282

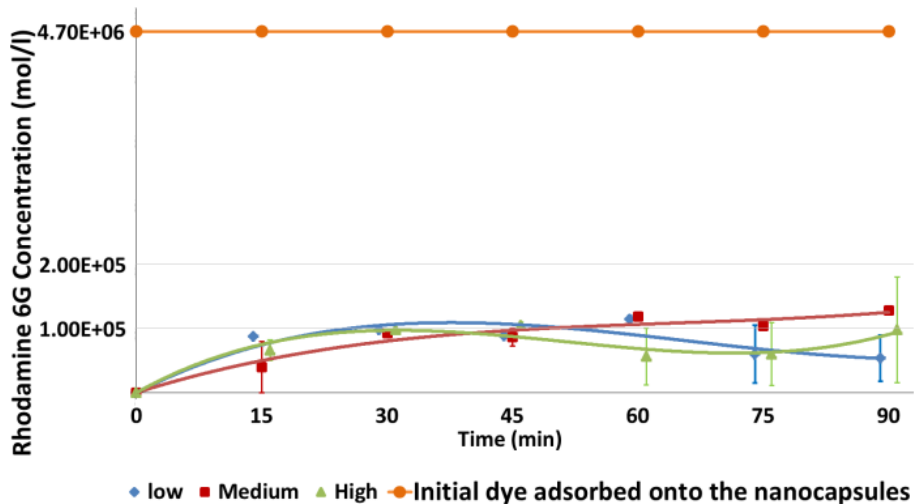
283 Figure 6. Rhodamine 6G concentration released from the capsules with gold nanoparticles against the ultrasonic stimulation
 284 time of the different duty cycles. The orange line represents the total concentration of Rhodamine 6G contained in the
 285 capsules.

286

287 The measurement was repeated twice independently in the collection of the presented in vitro data. The
 288 graph represents means with error bars for six times. Graph markers denote the data mean. The bars
 289 represent one standard deviation of the mean. Rhodamine 6G concentration in Figure 6 showed that
 290 samples after high-duty cycle ultrasonic stimulation carried out 6 times, 15 minutes each time, released
 291 more of the dye than under medium or low-duty cycle treatment. Little dye was released from these
 292 microcapsules after the first 15 minutes of the stimulation. Clear increases of Rhodamine 6G were
 293 observed after the second stimulation, although no significant differences were found among the different
 294 duty cycles. With the increase of the ultrasonic stimulation times, the Rhodamine 6G concentration
 295 further increased. This indicates that the ultrasonic treatment has a promoting effect on the dye release
 296 from the microcapsules with the gold nanoparticles. After the fourth (total 60 minutes) ultrasonic

297 treatment, the dye was still released from the samples. However, the rate of the Rhodamine 6G
298 concentration changes was reduced, particularly for the medium and low-duty cycle treatments. After the
299 sixth ultrasonic stimulation (90 minutes), the Rhodamine 6G concentration of the dye released from the
300 sample under the high-duty cycle treatment was close to the initial total intensity of the dye adsorbed
301 onto the microcapsules. This implies that most of the dye contained in the samples had been released. In
302 comparison, the Rhodamine 6G released from the samples with the medium or low-duty cycle of
303 ultrasound was lower than with the high-duty cycle. This means that there was still some dye in the
304 microcapsules. This is not surprising as the medium or low-duty cycle of ultrasound presented lower
305 power intensities than the high-duty cycle of ultrasound, causing a lower dye to be released from the
306 microcapsules. Nevertheless, the dye released from the microcapsules with ultrasonic stimulation was
307 still presented.

308
309 To study the influence of gold nanoparticles on the efficiency of the dye release, microcapsules without
310 gold nanoparticles in their shells were also synthesized and analyzed. Their results are shown in Figure 7.
311 The graph represents means with error bars for six times. Graph markers denote the data mean. The bars
312 indicate data range.



313

314

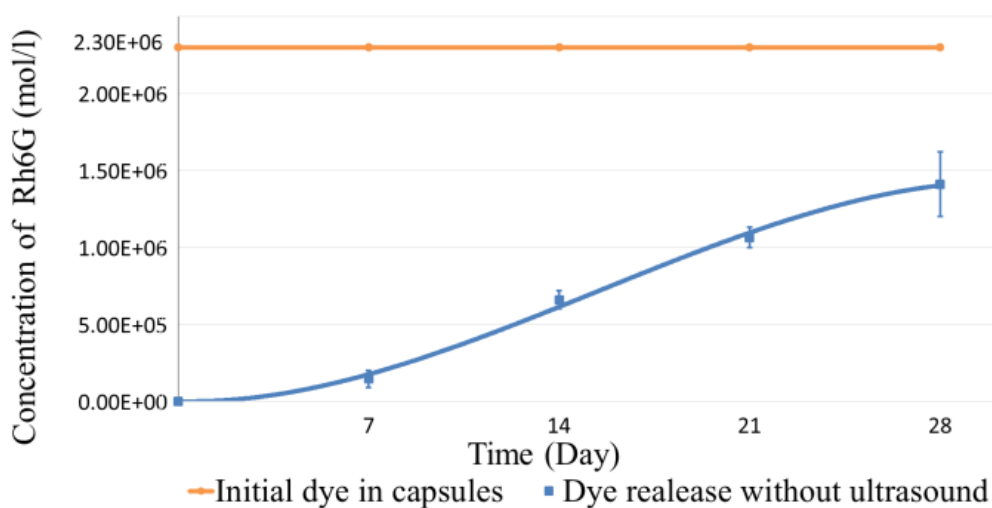
315 Figure 7. Rhodamine 6G concentration of the dye released from the capsules without gold nanoparticles measured after
316 various ultrasonic stimulation times of different duty-cycles.

317

318 It shows that there is no obvious changes in the concentration and R6G concentration is below 3% of the
319 total concentration after six cycles of stimulation. However, the change of fluorescence intensity with
320 the increase of the ultrasonic stimulation time was small. After the 6th stimulation, the concentration of
321 Rh6G was just 10% of the total initial concentration of Rh6G. Moreover, there was no significant
322 difference in the efficiency of the dye released by employing different duty cycles. It is thus clear that
323 gold nanoparticles in microcapsules play an important role in the ultrasonic induced release of dye.

324

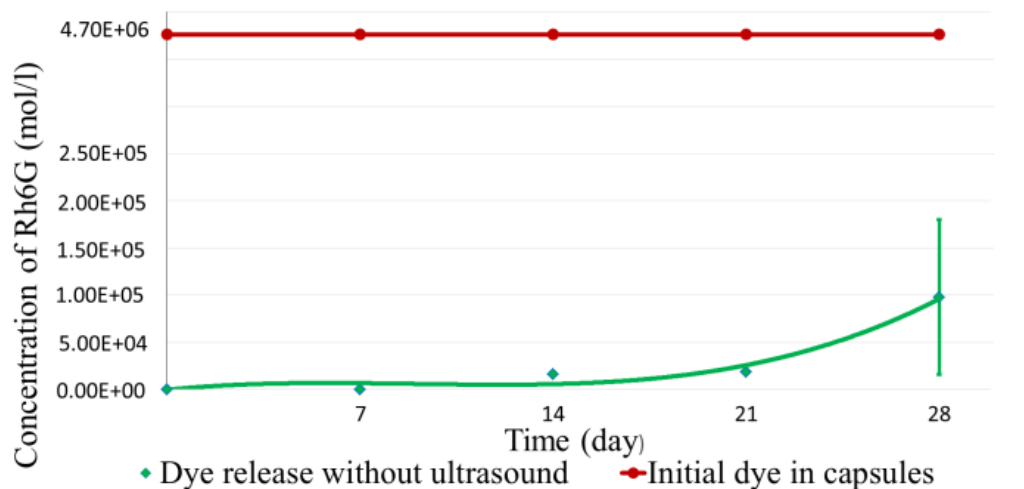
325 Finally, the release of dye from samples (1.5 ml) stored at room temperature at 200 without ultrasonic
326 treatment during a period of four weeks was also studied as a comparison. Both microcapsules with and
327 without gold nanoparticles were used in this study. Figure 8 shows the Rhodamine 6G concentration
328 changes of the dye released from microcapsules after a long period of storage at room temperature at 20
329 degrees.



330

331

(a)



(b)

332

333

334 Figure 8. Rhodamine 6G concentration of dye released from capsules (a) with and (b) without gold nanoparticles after room
 335 temperature storage (without any ultrasonic stimulation). The red line represents the Rhodamine 6G contained in the samples.

336

337 Figure 8 (a) shows that after an initial small release in the first week, a large amount of dye was released
 338 from microcapsules with gold nanoparticles in the following three weeks. The graph represents means
 339 with error bars for five times. Graph markers denotes the data mean. The bars indicate data range. In
 340 contrast, no obvious changes in the Rhodamine 6G concentration was observed in the case of
 341 microcapsules without gold nanoparticles for the first few weeks. The intensity of released dye after 4
 342 weeks was significantly weak compared to that from microcapsules with gold nanoparticles. This finding
 343 suggests that microcapsules containing gold nanoparticles are less stable compared to those without gold
 344 nanoparticles.

345

346

347 4. Discussion

348 In this study, the presence of gold nanoparticles allowed the dye to be released from PLA-
 349 Rh6G/PAH/PSS/PAH/AuNP/PAH microcapsules more efficiently, compared to microcapsules without

350 gold nanoparticles. According to these results, several factors may play a role in the stimulation process.
351 The presence of gold nanoparticles in the microcapsules makes the shells stiffer and lower in their
352 elasticity, which may have an effect on how easily the shells will move when applying an oscillating
353 force to them in liquid by means of ultrasonic stimulation. If they are moved, the rupturing may occur as
354 expected. As illustrated by Fery et al., the presence of inorganic nanoparticles increases the density
355 contrast of a microcapsule shell, which also decreases the elasticity of the shell. These are important for
356 achieving high efficiency in the ultrasonically treated release of compounds encapsulated in capsules
357 [39].

358
359 The effects of ultrasound as a release trigger may be attributed to acoustic cavitation in liquids under
360 ultrasonic vibrations with a frequency of more than 20 kHz. As demonstrated by Maria N. Antipina et al.,
361 ultrasound energy produces pressure and can cause the shrinkage of gas-filled nanobubbles. Then, the
362 cavitating nanobubbles implode, which produces local shock waves and destroy the nanocapsules
363 assemblies [40-44]. Even at low input power, the collapse of microbubbles in liquid results in an
364 enormous concentration of energy. When the capsules are subjected to ultrasonic stimulation, shear
365 forces between the successive fluid layers occurs, which leads to the disruption of the capsule assemblies
366 and the subsequent release of their payloads [39]. Therefore, acoustic cavitation resulted in dye release
367 from the nanocapsules in this study is a possible factor.

368
369 As for the nanocapsules without gold nanoparticles, they presented little dye release in this research. It
370 can be assumed that the capsules may be disrupted because of the absorption of intense energy of
371 ultrasound over a longer time. In previous research by academics, ultrasonic stimulation operating on the
372 capsules has been proven to produce heat. High temperature causes changes in permeability of the outer

373 shell and can even rupture the capsules. Subsequently, the release of capsules payload will be achieved
374 [45]. The heat produced by ultrasound may also have an influence on the dye released from samples
375 without gold nanoparticles.

376

377 **5. Conclusions**

378 This work aims to investigate a drug delivery system with stimuli-responsive polymeric microcapsules
379 that can achieve a locally controlled drug release by means of remote ultrasonic stimulation. The
380 microcapsules were synthesized with polyelectrolyte layers and gold nanoparticles by means of a layer-
381 by-layer assembly technique, encapsulated with a model dye used in place of anti-restenotic drugs. The
382 microcapsules with and without gold nanoparticles embedded in the shell were examined for their
383 response to ultrasonic stimulation. The presence of gold nanoparticles significantly enhances the
384 efficiency of the ultrasonically induced dye release from the microcapsules. It is shown that the
385 microcapsules containing gold nanoparticles are more sensitive to ultrasonic treatment compared with the
386 microcapsules without gold nanoparticles. Such a method will give the interventional cardiologist more
387 control over the medical implants.

388

389 **Declarations**

390 Interests conflict: None

391 Funding: None

392 Ethical approval: Not required

393

394 **6. References**

395 [1] Alwan A. World Health Organization. Global Status Report on Noncommunicable Diseases 2010,
396 2011.
397

- 398 [2] Otsuka F, Finn AV, Yazdani SK, Nakano M, Kolodgie FD, Virmani R. The importance of the
399 endothelium in atherothrombosis and coronary stenting , *Nat Rev Cardiol* 2012;9: 439-53.
- 400 [3] Acharya G, Park K. Mechanisms of controlled drug release from drug-eluting stents. *Adv Drug*
401 *Deliv Rev* 2006;58: 387-401.
- 402 [4] Sprague EA, Tio F, Ahmed SH, Granada JF, Bailey SR. Impact of parallel micro-engineered stent
403 grooves on endothelial cell migration, proliferation, and function: an in vivo correlation study of the
404 healing response in the coronary swine model. *Circ Cardiovasc Interv* 2012; 5: 499-507.
- 405 [5] Steigerwald K, Ballke S, Quee SC, Byrne RA, Vorpahl M, Vogeser M, Kolodgie F, Virmani R,
406 Joner M. Vascular healing in drug-eluting stents: differential drug-associated response of limus-eluting
407 stents in a preclinical model of stent implantation. *EuroIntervention* 2012;8:752-9.
- 408 [6] Ito S, Nakasuka K, Sekimoto S, Miyata K, Inomata M, Yoshida T & Sato K. Intracoronary Imaging
409 and Histopathology of Late Phase In-Stent Restenosis after Coronary Stent Implantation. *ISRN Vascular*
410 *Medicine* 2012; Article ID 678137, 11 pages. <http://dx.doi.org/10.5402/2012/678137>
- 411 [7] Kiran U, Makhija N. Patient with recent coronary artery stent requiring major non cardiac surgery.
412 *Indian J Anaesth* 2009; 53(5): 582.
- 413 [8] Ma WJ, Yuan XB, Kang CS, Su T, Yuan XY, Pu PY, Sheng J. Evaluation of blood circulation of
414 polysaccharide surface-decorated PLA nanoparticles. *Carbohydr Polym* 2008; 72(1): 75-8.
- 415 [9] Reed AM, Gilding DK. Biodegradable polymers for use in surgery—poly (glycolic)/poly (lactic acid)
416 homo and copolymers: 2. In vitro degradation. *Polymer* 1981; 22(4): 494-498.
- 417 [10] Anderson JM, Shive MS. Biodegradation and biocompatibility of PLA and PLGA microspheres.
418 *Adv. Drug Deliv Rev* 2012; 64:72-82.
- 419 [11] Couvreur P, Vauthier C. Nanotechnology: intelligent design to treat complex disease. *Pharm Res*
420 2006; 23(7): 1417-1450.

- 421 [12] Borges J, Rodrigues LC, Reis RL, Mano JF. Layer-by-layer assembly of light-responsive polymeric
422 multilayer systems. *Adv Funct Mater* 2014; 24(36): 5624-564.
- 423 [13] Jain S, Hirst DG, O'sullivan JM. Gold nanoparticles as novel agents for cancer therapy. *Br J Radiol*
424 2012; 85(1010):101-13.
- 425 [14] Huang X, El-Sayed MA., Gold nanoparticles: optical properties and implementations in cancer
426 diagnosis and photothermal therapy. *Int j adv res* 2010; 1(1):13-28.
- 427 [15] Pavlov AM, Saez V, Cobley A, Graves J, Sukhorukov GB, Mason TJ. Controlled protein release
428 from microcapsules with composite shells using high frequency ultrasound—potential for in vivo
429 medical use. *Soft Matter* 2011; 7(9):4341-4347.
- 430 [16] Antipina MN, Sukhorukov GB. Remote control over guidance and release properties of composite
431 polyelectrolyte based capsules. *Adv Drug Deliv Rev* 2011; 63(9): 716–29.
- 432 [17] Skrabalak SE, Chen J, Sun Y, Lu X, Au L, Cobley CM, Xia Y. Gold nanocages: synthesis,
433 properties, and applications. *Acc Chem Res* 2008; 41(12): 1587-1595.
- 434 [18] Yu YY, Chang SS, Lee CL, Wang CC. Gold nanorods: electrochemical synthesis and optical
435 properties. *J Phys Chem B* 1997;101(34): 6661-6664.
- 436 [19] Kost J, & Langer R. Responsive polymer systems for controlled delivery of therapeutics. *Trends*
437 *Biotechnol* 1992;10:127-131.
- 438 [20] Zhao YZ, Du LN, Lu CT, Jin YG, Ge SP. Potential and problems in ultrasound-responsive drug
439 delivery systems. *Int J Nanomedicine* 2013; 8:1621-1633.
- 440 [21] Norris P, Noble M, Francolini I, Vinogradov AM, Stewart PS, Ratner BD, Stoodley P.
441 Ultrasonically controlled release of ciprofloxacin from self-assembled coatings on poly (2-hydroxyethyl
442 methacrylate) hydrogels for *Pseudomonas aeruginosa* biofilm prevention. *Antimicrob Agents Chemother*
443 2005; 49(10):4272-4279.

- 444 [22] Lentacker I, De Geest BG, Vandenbroucke RE, Peeters L, Demeester J, De Smedt SC, Sanders N.
445 Ultrasound-responsive polymer-coated microbubbles that bind and protect DNA. *Langmuir* 2006;22(17):
446 7273-7278.
- 447 [23] Marmottant P, & Hilgenfeldt S. Controlled vesicle deformation and lysis by single oscillating
448 bubbles, *Nature* 2003;423(6936): 153-156.
- 449 [24] Kost J, Leong K, Langer R. Ultrasound-enhanced polymer degradation and release of incorporated
450 substances. *Proc Natl Acad Sci U.S.A* 1989; 86(20):7663-7666.
- 451 [25] Kost J, Leong K, Langer R. Ultrasonic modulated drug delivery systems. In *Polymers in Medicine*
452 *II*, Springer ;1986, p. 387-396.
- 453 [26] Lavon I, Kost J. Mass transport enhancement by ultrasound in non-degradable polymeric controlled
454 release systems. *J Control Release* 1998; 54(1): 1-7.
- 455 [27] Liu LS, Kost J, D'Emanuele A, Langer R. Experimental approach to elucidate the mechanism of
456 ultrasound-enhanced polymer erosion and release of incorporated substances. *Macromolecules* 1992;
457 25(1): 123-128.
- 458 [28] Kost J, Leong K, Langer R. Ultrasonically controlled polymeric drug delivery. In: *Macromolecular*
459 *Symposia* , Hüthig & Wepf Verlag; 1998, p. 275-285 .
- 460 [29] Kost J, Liu LS, Gabelnick H, Langer R. Ultrasound as a potential trigger to terminate the activity of
461 contraceptive delivery implants. *J Control Release* 1994; 30(1): 77-81.
- 462 [30] Miyazaki S, Yokouchi C, Takada M. External control of drug release: controlled release of insulin
463 from a hydrophilic polymer implant by ultrasound irradiation in diabetic rats. *J Pharm Pharmacol*
464 1998;40(10): 716-717.
- 465 [31]Miyazaki S, Hou WM, Takada M. Controlled drug release by ultrasound irradiation. *Chem Pharm*
466 *Bull* 1985; 33(1): 428-431.

467 [32] Chen F, Ma M, Wang J, Wang F, Chern SX, Zhao ER, Jhunhunwala A, Darmadi S, Chen H,
468 Jokerst JV. Exosome-like silica nanoparticles: a novel ultrasound contrast agent for stem cell imaging.
469 *Nanoscale* 2017; 9 (1): 402-411.

470 [33] Chen F, Zhao E, Kim T, Wang J, Hableel J, Reardon P, Ananthakrishna SJ, Wang T, Arconada-
471 Alvarez S, Knowles JC and Jokerst JV. Organosilica Nanoparticles with an Intrinsic Secondary Amine:
472 An Efficient and Reusable Adsorbent for Dyes. *ACS Appl. Mater. Interfaces*, 2017, 9 (18):15566–15576.

473 [34] El Fagui A, Dalmas F, Lorthioir C, Wintgens V, Volet G, Amiel C. Well-defined core-shell
474 nanoparticles containing cyclodextrin in the shell: a comprehensive study. *Polymer* 2011; 52(17): 3752-
475 3761.

476 [35] Grabar KC, Freeman RG, Hommer MB, Natan MJ. Preparation and Characterization of Au Colloid
477 Monolayers. *Anal Chem* 1995; 67: 735–743.

478 [36] Apfel RE, Holland CK. Gauging the likelihood of cavitation from short-pulse, low-duty cycle
479 diagnostic ultrasound. *Ultrasound Med Biol* 1991;17(2): 179-185.

480 [37] Hendee WR, Ritenour ER. Medical imaging physics. John Wiley & Sons; 2003.

481 [38] El Fagui A, Wintgens V, Gaillet C, Dubot P, Amiel C. Layer-by-Layer Coated PLA Nanoparticles
482 with Oppositely Charged β -Cyclodextrin Polymer for Controlled Delivery of Lipophilic Molecules.
483 *Macromol Chem Phys* 2014; 215(6): 555-565.

484 [39] Dubreuil F, Shchukin DG, Sukhorukov GB, Fery A. Polyelectrolyte capsules modified with YF3
485 nanoparticles: an AFM study. *Macromol Rapid Co* 2004; 25(11):1078-1081.

486 [40] Rae J, Ashokkumar M, Eulaerts O, von Sonntag C, Reisse J, Grieser F. Estimation of ultrasound
487 induced cavitation bubble temperatures in aqueous solutions. *Ultrason Sonochem* 2005; 12(5): 325-329.

488 [41] Shchukin DG, Gorin DA, Möhwald H. Ultrasonically induced opening of polyelectrolyte
489 microcontainers. *Langmuir* 2006; 22(17):7400-740.

- 490 [42] Skirtach AG, De Geest BG, Mamedov A, Antipov AA, Kotov NA, Sukhorukov GB. Ultrasound
491 stimulated release and catalysis using polyelectrolyte multilayer capsules. *J Mater Chem* 2007;
492 17(11):1050-1054.
- 493 [43] De Geest BG, Skirtach AG, Mamedov AA, Antipov AA, Kotov NA, De Smedt SC, Sukhorukov
494 GB. Ultrasound-Triggered Release from Multilayered Capsules. *Small* 2007; 3(5): 804-808.
- 495 [44] Kolesnikova TA, Gorin DA, Fernandes P, Kessel S, Khomutov GB, Fery A, Möhwald H.
496 Nanocomposite microcontainers with high ultrasound sensitivity. *Adv Funct Mater* 2010;20(7):1189-
497 1195.
- 498 [45] Skirtach AG, Dejugnat C, Braun D, Susha AS, Rogach AL, Parak WJ, Sukhorukov G B. The role of
499 metal nanoparticles in remote release of encapsulated materials. *Nano Lett* 2005; 5(7): 1371-1377.